PHYSICAL REVIEW B

CONDENSED MATTER AND MATERIALS PHYSICS

THIRD SERIES, VOLUME 60, NUMBER 6 1 AUGUST 1999-II

RAPID COMMUNICATIONS

Rapid Communications are intended for the accelerated publication of important new results and are therefore given priority treatment both in the editorial office and in production. A Rapid Communication in **Physical Review B** *may be no longer than four printed pages and must be accompanied by an abstract. Page proofs are sent to authors.*

Microscopic analysis of the laser-induced femtosecond graphitization of diamond

H. O. Jeschke, M. E. Garcia, and K. H. Bennemann
Institut für Theoretische Physik der Freien Universität Berlin, Arnimallee 14, D-14195 Berlin, Germany
(Received 8 March 1999; revised manuscript received 21 April 1999)

We present a theoretical study of ultrafast phase transitions induced by femtosecond laser pulses of arbitrary form. Molecular-dynamics simulations on time dependent potential-energy surfaces derived from a microscopic Hamiltonian are performed. Applying this method to diamond, we show that a nonequilibrium transition to graphite takes place for a wide range of laser pulse durations and intensities. This ultrafast transition ($\sim$100 fs) is driven by the suppression of the diamond minimum in the potential-energy surface of the laser excited system. [S0163-1829(99)50730-3]

The understanding of the mechanisms for ultrafast nonequilibrium phase transitions is a fundamental problem in solid-state physics. In the last years several laser-induced ultrafast phase transitions have been observed, which open the possibility for the study of qualitatively new effects.[1–7] Particularly interesting are laser-induced ultrafast transitions between two crystalline structures, about which little is known at present.

In this paper we present calculations of a nonthermal, femtosecond graphitization of diamond as an example for a nonequilibrium phase transition between two crystalline phases induced by an ultrafast laser excitation of electrons. We develop a computational approach to treat electronic effects in molecular-dynamics (MD) simulations with multiple potential-energy surfaces. We describe excitation of electrons with a laser pulse of arbitrary shape and energy, taking into account explicitly electron thermalization and diffusion effects.

Note that recent theoretical studies of the diamond graphitization describe a thermally induced transition with electrons and lattice in thermodynamical equilibrium.[8] On the other hand, the ultrafast melting of solids via laser irradiation was theoretically analyzed under the assumption that the volume remains constant along the transition path.[9–11]

In contrast, we analyze the laser-induced graphitization of diamond by allowing volume changes, since crystalline diamond and graphite have rather different densities. Our study concentrates on a subregion of volume $\Omega_{sr}\sim 10^6$ Å^3 in the center of the much larger irradiated volume ($\Omega_{irr}\sim 10^{13}$ Å^3). In the subregion, which we simulate by a MD supercell ($\Omega_{MD}\sim 10^3$ Å^3) using periodic boundary conditions, nearly homogeneous rapid volume and shape changes are expected upon excitation.

Our physical picture for the nonequilibrium dynamics of the considered MD supercell of diamond is the following. Due to the action of the laser pulse, electrons are excited from occupied to unoccupied levels with a time-dependent probability which is proportional to the intensity of the laser field. As a consequence of the extremely fast excitation process, a nonequilibrium distribution of electrons is created. Through electron-electron collisions this electron distribution thermalizes to an equilibrium occupation of the electronic levels. Simultaneously, hot-electron transport from the excited region into the rest of the material sets in. During this complex electron dynamics the lattice undergoes a restructuring process in response to the dramatic changes in the potential-energy surface (PES). These structural changes may lead to another crystal phase.

In view of the above discussion and in order to allow deformations and expansions of the MD supercell, we perform simulations at constant pressure,[12,13] which are based upon a Lagrangian of the form

$$L(t)=\sum_{i=1}^{N}\frac{m_i}{2}\,\dot{\mathbf{s}}_i^T h^T h\dot{\mathbf{s}}_i-\sum_{\substack{i=1\\ j\neq i}}^{N}\Phi(r_{ij},t)+K-P\Omega. \qquad (1)$$

Here, the coordinates $\mathbf{s}_i$ of the N atoms are taken relative to the vectors **a**, **b**, and **c** that form the MD supercell and constitute the matrix $h=(\mathbf{abc})$. The absolute coordinates of the atoms are given by $\mathbf{r}_i=h\mathbf{s}_i$. $\Omega=\det(h)$ is the volume of the

MD supercell and P is the external pressure. The second term represents the PES, which is determined from a microscopic theory as described below. The third and fourth terms of the Lagrangian are introduced to simulate the time evolution of the MD unit cell.[12,13] The third term K describes the kinetic energy of the MD supercell.[14,15] Using the Euler-Lagrange formalism, $N+9$ equations of motion for the atomic coordinates $\mathbf{s}_i$ and for the MD cell coordinates h_{kl} are derived from Eq. (1).[12,13]

The forces which enter the equations of motion as $d\Phi(r_{ij})/d\mathbf{s}_k$ are determined using the Born-Oppenheimer approximation and the Hellmann-Feynman theorem and are given by

$$\mathbf{f}_i = -\sum_m n(\varepsilon_m,t)\left\langle m\left|\frac{\partial H}{\partial \mathbf{s}_i}\right|m\right\rangle - \frac{\partial E_{\mathrm{rep}}}{\partial \mathbf{s}_i}, \tag{2}$$

where m labels the electronic levels, which are the eigenstates of the electronic Hamiltonian $H(\mathbf{r}_1,\cdots,\mathbf{r}_N)$. $E_{rep}(\mathbf{r}_1,\cdots,\mathbf{r}_N)$ contains the repulsive interactions between the atomic cores. The forces for the MD supercell h result in close analogy.[12,13] In Eq. (2) $n(\varepsilon_m,t)$ refers to the occupation of the energy level ε_m at time t, which changes due to the action of the laser pulse, Coulomb interactions, and diffusion effects. $n(\varepsilon_m,t)$ is initially given by a Fermi distribution at the temperature of the lattice. During the excitation by the laser pulse, this distribution changes in time according to

$$\frac{dn(\varepsilon_m,t)}{dt} = \int_{-\infty}^{\infty} d\omega g(\omega,t-\Delta t)\{[n(\varepsilon_m-\hbar\omega,t-\Delta t) + n(\varepsilon_m+\hbar\omega,t-\Delta t)-2n(\varepsilon_m,t-\Delta t)]\} - \frac{n(\varepsilon_m,t)-n^0(\varepsilon_m)}{\tau_1}. \tag{3}$$

Here, the first term describes the laser-induced excitation processes $\varepsilon_m \rightarrow \varepsilon_m \pm \hbar\omega$ which are weighted by the spectral function $g(\omega,t)$ of the laser pulse at each time step Δt. The second term of Eq. (3) takes into account, in a simple approximation, the thermalization processes due to electron-electron collisions. The nonequilibrium distribution $n(\varepsilon_m,t)$ relaxes towards a Fermi distribution $n^0(\varepsilon_m)=2/\{\exp[(\varepsilon_m-\mu)/k_BT_e(t)]+1\}$ with a time constant τ_1.

The time-dependent electron temperature $T_e(t)$ contained in $n^0(\varepsilon_m)$ is obtained from the time evolution of the total energy

$$E_t(t)=\sum_{\substack{i=1\\ j\neq i}}^{N}\Phi(r_{ij},t)+E_{kin}(t)=E_t(0)+E_{abs}(t), \tag{4}$$

where $E_{kin}(t)$ is the kinetic energy of the atoms and $E_{abs}(t)$ is the energy that has already been absorbed from the laser pulse at time t. The PES is determined by $\sum_{i=1}^{N}\sum_{j\neq i}\Phi(r_{ij},t)=\sum_m n(\varepsilon_m,t)\varepsilon_m(\mathbf{r}_1,\ldots,\mathbf{r}_N)$, where ε_m are the eigenvalues of the Hamiltonian

$$H=\sum_{i\alpha}\epsilon_{i\alpha}n_{i\alpha}+\sum_{\substack{ij\alpha\beta\\ j\neq i}}V_{ij}^{\alpha\beta}(r_{ij})c_{i\alpha}^{+}c_{j\beta}. \tag{5}$$

Here, $\epsilon_{i\alpha}$ is the on-site energy of atom i and orbital α. $c_{i\alpha}^{+}$ and c_{jp} are the creation and annihilation operators, and

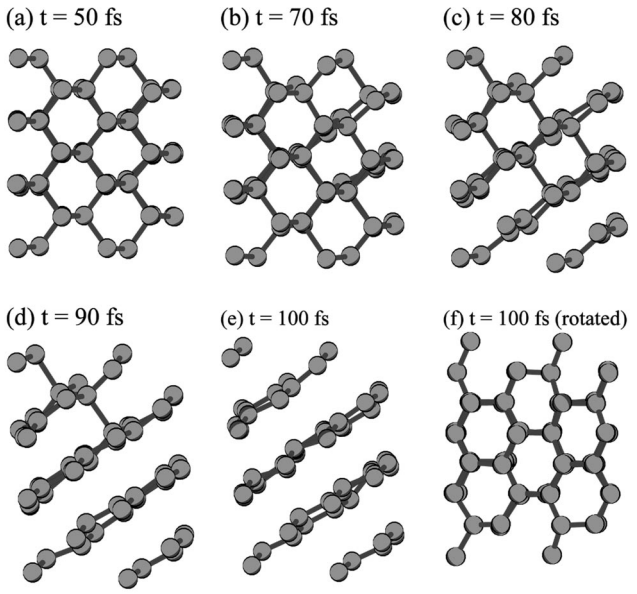

FIG. 1. Snapshots in the (110) direction of the ultrafast dynamics of diamond ($N=64$ atoms) upon excitation with a laser pulse of duration $\tau=20$ fs (Gaussian shape). t is the time delay with respect to the peak of the pulse. The energy absorbed is $E_{abs}=1.3$ eV/atom. (f) View along an axis perpendicular to the graphite layers formed after 100 fs. Bonds longer than 1.6 Å are not shown.

$V_{ij}^{\alpha\beta}(r_{ij})$ the hopping integrals. For the description of carbon, the $2s$, $2p_x$, $2p_y$, and $2p_z$ orbitals are taken into account. For the radial part of the hopping integrals and for E_{rep} we employ the functions proposed by Xu *et al.* (Ref. 16).

At the short time scale of a few picoseconds, the main process causing dissipation of the absorbed energy is the diffusion of hot electrons into the surrounding cold lattice. This is taken into account by a further rate equation $dT_e(t)/dt=-[T_e(t)-T_l(t)]/\tau_2$, i.e., within a diffusion time constant τ_2 the electron temperature $T_e(t)$ approaches the lattice temperature $T_l(t)$.

The time evolution of the system after excitation with a pump pulse is usually studied experimentally by measuring the reflectivity with the help of a probe pulse as a function of the pump-probe delay. Thus, in order to compare with experiment or to make predictions we estimate the time-dependent dielectric function from $\epsilon(\omega,t)=\epsilon_{GS}(\omega,t)+\epsilon_p(\omega,t)$, where ω is the frequency of the probe pulse. ϵ_{GS} refers to the dielectric function for the ground state of diamond,[17] whereas ϵ_p corresponds to the contribution of the excited electrons under the assumption that the electron-hole plasma shows metallicliike behavior.[18] From this dielectric function the reflectivity R is calculated in the standard way.[19]

We have performed the MD simulations using diamond super cells consisting of $N=64$ and $N=216$ atoms, and periodical boundary conditions.[20] The derivatives of the matrix elements of $H(\mathbf{r}_1,\cdots,\mathbf{r}_N)$ and of the repulsive potential E_{rep} are calculated analytically. The equations of motion are integrated using the Verlet algorithm.

We characterize the laser pulse by a Gaussian of duration τ and by the quantity E_{abs}, which is the energy absorbed by the system and is proportional to the intensity of the pulse. Since we do not include multiphoton effects we set the fre-

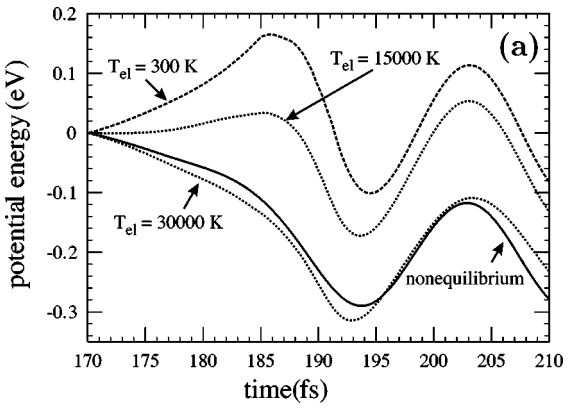

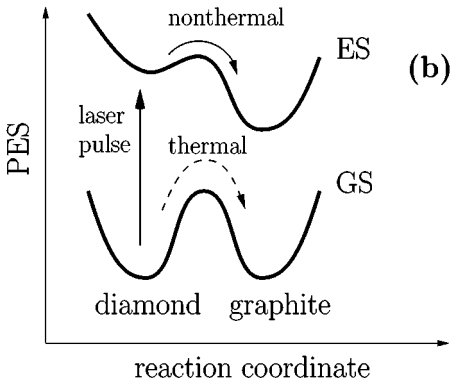

FIG. 2. (a) Potential energy as a function of time upon excitation with a laser pulse of $\tau=100$ fs and absorbed energy $E_{abs}=1.3$ eV/atom (solid line). The dashed lines refer to the potential energy along the same graphitization path but calculated by assuming different electronic temperatures. For $T_e=300$ K the energy barrier between diamond and graphite is 0.17 eV/atom. (b) Illustration of the mechanism for the laser-induced nonequilibrium graphitization of diamond as suggested by (a). GS and ES refer to the ground state and excited state, respectively. The dashed arrow indicates graphitization occurring for thermodynamical equilibrium.

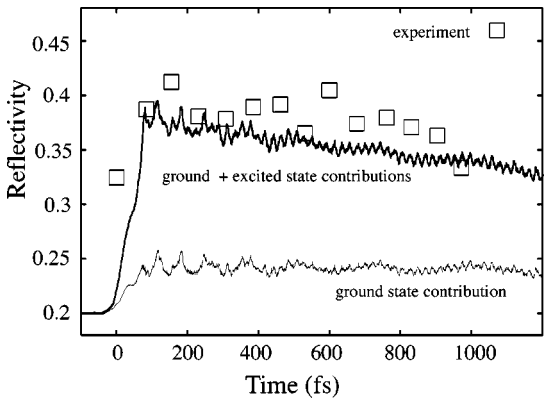

FIG. 3. Time evolution of the reflectivity R for $\hbar\omega=2$ eV. Squares correspond to the experimental results of Ref. 3. The thick line refers to the excited electrons, the thin line to the ground-state contribution (see Ref. 17). The parameters used were $\tau=50$ fs, $E_{abs}=1.35$ eV/atom (corresponding to a fluence of 1.1 J/cm^2), and $\gamma=1.43\times10^{14}$ s^{-1} (see Ref. 18). The comparison with experiment is only qualitative, since the experimental data refer to laser-induced melting.

quency of the pump pulse to be $\omega_{pump}=6$ eV, i.e., larger than the energy gap of diamond.

We investigate the response of diamond to laser pulses for different values of τ and E_{abs}. Below the ablation threshold (which we define by the complete destruction of the diamond cell) we obtain, for all pulse durations investigated ($\tau=20-500$ fs) and for absorbed energies E_{abs} ranging from $E_{abs}=1$ eV/atom to $E_{abs}=2.5$ eV/atom an ultrafast graphitization of the initial diamond structure.

In Fig. 1 we show, for given values of τ and E_{abs}, the ultrafast graphitization in the (110) direction of the diamond crystal. The 64-atom sample of diamond was excited by a 20 fs laser pulse, and the Figs. 1(a)–(e) show the structural changes at different times: the bent hexagons of the diamond lattice in the (110) direction break up to form the even planes of graphite, while in the direction perpendicular to the newly formed planes the originally bent hexagons become flat and form the even hexagons of the graphite lattice [see Fig. 1(f)]. Note, that in this freshly formed graphite lattice, which is in a high vibrational excitation, the planes are still all equivalent, and the familiar structure of hexagonal and rhombohedral graphite with layering sequences of *ABABAB* and *ABCABC*, respectively, has not yet been formed. Although it is to be expected that the system will eventually transform towards one of these two standard structures of graphite, in the tight binding method no energy difference between different layer arrangements is observed because the interplane van der Waals interactions are not taken into account. The graphite structure remains intact until our maximal simulation time $t=5$ ps. However, we believe that further relaxation leads to a disordered graphite lattice, which can probably only be described using very large MD super cells. It is important to point out that, although we allow volume expansions in all directions, these only occur in the direction perpendicular to the newly formed graphite planes. Note that our volume expansions upon graphitization relate to the considered subregion due to our use of a MD super cell with periodic boundary conditions. While the electronic transition $sp^3\rightarrow sp^2$ behind the graphitization occurs very fast (in less than 50 fs), the time scale for the following volume and shape changes is characterized by the velocity of typically $v_{cp}\approx0.03$ Å/fs, which may be compared with the velocity of sound in diamond, $c_D=0.18$ Å/fs.

We found that the time scale for the collective atomic motion shown in Fig. 1 is independent of the size used for the MD super cell ($N=64$ and $N=216$), and thus the size chosen is large enough. Furthermore, as long as the subregion studied is much smaller than the laser irradiated region ($\Omega_{irr}\sim10^{13}$ Å^3), our assumption of homogeneous volume and shape changes of the subregion should be valid and the effects due to the interface between the laser excited and the cold material should be negligible.

In Fig. 2(a) the influence of the laser-induced electron-hole excitations on the potential-energy barrier between diamond and graphite is analyzed. Along the graphitization path obtained by a 100 fs, 1.3 eV/atom laser pulse we plot the PES corresponding to occupations $n(\varepsilon_m,t)$ at electronic temperatures $T_e=300$ K (ground state), $T_e=15000$ K, and $T_e=30000$ K (highly excited states). The abscissa has the meaning of a time scale for the curve corresponding to the actual electron-hole plasma causing this trajectory, while for the other PES's it corresponds to the reaction coordinate.

In Fig. 2(b) we illustrate schematically the microscopic mechanism of the nonequilibrium ultrafast graphitization of diamond as follows from Fig. 2(a). Before the action of the femtosecond laser pulse both the structure of graphite and that of diamond correspond to deep minima of the PES and are well separated by a high potential barrier [see Fig. 2(a) for $T_e=300$ K]. However, for increasing energy E_{abs} absorbed by the electronic system the minimum corresponding to the diamond structure becomes weaker, and for a critical E_{abs} it disappears [see Fig. 2(a) for $T_e=15000$ K and $T_e=30000$ K, respectively]. In contrast, the graphite minimum of the excited PES is less sensitive to the creation of electron-hole pairs and remains stable. This results physically from the different binding character in graphite and diamond. As a consequence of the sp^2 hybridization in graphite, the electrons in the $2p_z$ orbitals of carbon are not essential for the stability of the bonds and can thus be excited into antibonding states without destruction of the structure. Now, due to their large DOS below and above the Fermi level a large part of the laser excited electron-hole pairs belong to the $2p_z$ symmetry. In the sp^3-hybridized diamond bond, however, all valence electrons are in the same way responsible for stability, and excitation immediately weakens the cohesion of the diamond lattice. The trajectory followed by the system during the transition is strongly dependent on the pulse duration and intensity. For instance, the potential-energy barrier in the excited state shown in Fig. 2(a) is lower than that obtained using a laser pulse of duration $\tau=20$ fs. In order to contrast this new nonequilibrium transition with previous studies we also indicate in Fig. 2(b) a path for the known equilibrium graphitization as described by DeVita *et al.*[8] where the energy barrier between diamond and diamond structures is overcome by thermal activation.

We have determined $\epsilon(\omega,t)$ and the reflectivity $R(t)$ for $\hbar\omega=2$ eV which simulates the response to a probe pulse of 620 nm wavelength. The result for $R(t)$ is shown in Fig. 3. Note, that the short time behavior of $R(t)$ is dominated by the contribution of the excited electrons and thus does not contain sufficient information to distinguish between different phases obtained by graphitization or melting, for example. However, since the free electrons in the conduction band play the essential role, we expect similar behavior of $R(t)$ for graphitization or melting. Thus, in the absence of data for ultrafast graphitization, we compare with experiments referring to melting of diamond at a fluence of 5.5 J/cm^2.[3]

We have also performed calculations without the third and fourth terms in the Lagrangian (Eq. 1) by studying the femtosecond laser excitation of a diamond film.[21] For the simulation of such a film we considered a MD super cell of 320 atoms with rigid boundary conditions in the horizontal directions and vacuum in the perpendicular direction (111) as used in Ref. 8. These calculations confirm the constant pressure results presented in Figs. 1–3, namely, rapid graphitization and volume expansions due to the repulsion of the graphite planes. For the film, the time scale of the volume change is characterized by the velocity of $v_f\approx 0.05$ Å/fs (v_f is larger than v_{cp}). This result supports our belief that we gained insight into the basic mechanism of nonequilibrium graphitization on a femtosecond time scale already by assuming constant pressure.

Summarizing, we presented a theoretical approach to calculate the nonequilibrium graphitization of diamond induced by a laser pulse. We believe that the mechanism for nonequilibrium phase transitions shown in Fig. 2(b) is quite general and could be applied to other laser-induced structural transformations.

This work was supported by the Deutsche Forschungsgemeinschaft through SFB 450.

[1] H. W. K. Tom *et al.*, Phys. Rev. Lett. **60**, 1438 (1988).
[2] K. Sokolowski-Tinten *et al.*, Phys. Rev. B **51**, 14 186 (1995) and references therein.
[3] D. H. Reitze *et al.*, Phys. Rev. B **45**, 2677 (1992).
[4] T. Dallas *et al.*, Phys. Rev. B **49**, 796 (1994); S. Preuss and M. Stuke, Appl. Phys. Lett. **67**, 338 (1995).
[5] I. L. Shumay and U. Höfer, Phys. Rev. B **53**, 15 878 (1996).
[6] P. Saeta *et al.*, Phys. Rev. Lett. **67**, 1023 (1991); L. Huang *et al.*, *ibid.* **80**, 185 (1998).
[7] J. Solis *et al.*, Phys. Rev. Lett. **76**, 2519 (1996); K. Sokolowski-Tinten *et al.*, *ibid.* **81**, 3679 (1998).
[8] A. De Vita *et al.*, Nature (London) **379**, 523 (1996).
[9] P. Stampfli and K. H. Bennemann, Phys. Rev. B **42**, 7163 (1990); **49**, 7299 (1994).
[10] P. L. Silvestrelli *et al.*, Phys. Rev. Lett. **77**, 3149 (1996); P. L. Silvestrelli and M. Parrinello, J. Appl. Phys. **83**, 2478 (1998).
[11] S. Das Sarma and J. R. Senna, Phys. Rev. B **49**, 2443 (1994).
[12] H. C. Andersen, J. Chem. Phys. **72**, 2384 (1980).
[13] M. Parrinello and A. Rahman, J. Appl. Phys. **52**, 7182 (1981).
[14] C. L. Cleveland, J. Chem. Phys. **89**, 4987 (1988).
[15] In the original theory of Parrinello and Rahman (Ref. 13) the third term is written as $K_{PR}=1/2W\mathrm{Tr}(\dot{h}^T\dot{h})$, whereas the improved version due to Cleveland (Ref. 14), which is independent of the choice of the MD super cell, reads $K_C=1/2W\mathrm{Tr}(\dot{h}\sigma^T\sigma\dot{h}^T)$ with $\sigma_{\alpha\beta}=\partial\Omega/\partial h_{\alpha\beta}$. We used both approaches and obtained identical results. W is a parameter with the dimension of mass.
[16] For more details see C. H. Xu *et al.*, J. Phys.: Condens. Matter **4**, 6047 (1992).
[17] We approximate ϵ_{GS} by $\epsilon_{GS}(\omega,t)=1+A\Sigma_{mm'}[n(\varepsilon_m,t)-n(\varepsilon_{m'},t)]/[\hbar\omega-\varepsilon_m(t)+\varepsilon_{m'}(t)+i\Gamma]$. The parameter A can be fitted in order to reproduce the equilibrium reflectivity of diamond.
[18] $\epsilon_p(\omega,t)=-\omega_p(t)(\omega^2+\gamma^2)+i\omega_p(t)\gamma/(\omega^3+\omega\gamma^2)$, where ω_p is the plasma frequency of the excited electrons and γ is the inverse plasmon relaxation time.
[19] J. P. Mathieu, *Optics* (Pergamon Press, Oxford, 1975).
[20] We adjusted W so that the fluctuations of the MD cell volume Ω, in the electronic ground state of the system, take place on a time scale of $\sqrt[3]{\Omega}/c_M$, where c_M is the speed of sound in the material (see Ref. 12).
[21] Further results will be published elsewhere as a review.